Journal of Hazardous Materials 175 (2010) 179–186

Contents lists available at ScienceDirect

Journal of Hazardous Materials

journal homepage: www.elsevier.com/locate/jhazmat

Preparation of dye waste-barium sulfate hybrid adsorbent and application in organic wastewater treatment

Zhang-Jun Hu, Yan Xiao, Dan-Hua Zhao, Yu-Lin Shen, Hong-Wen Gao*

State Key Laboratory of Pollution Control and Resources Reuse, College of Environmental Science and Engineering, Tongji University, Siping Rd 1239, Shanghai 200092, PR China

ARTICLE INFO

Article history:
Received 17 July 2009
Received in revised form
26 September 2009
Accepted 28 September 2009
Available online 2 October 2009

Keywords:
Hybridization
Dye wastewater
Barium sulfate
Sorbent
Organic wastewater

ABSTRACT

A new hybrid material was developed by the template-free hybridization of weak acidic pink red B (APRB, C.I. 18073) with $BaSO_4$. The composition and structure of the material were determined and characterized. In contrast to conventional sorbents, the hybrid material has a specific surface area of 0.89 m^2/g, but it contains lots of negative charges and lipophilic groups as the basis of specific adsorption. The efficient removal of cationic dyes and persistent organic pollutants (POPs) indicates that it has an improved adsorption capacity and selectivity with a short removal time less than 2 min; while the hybrid sorbents fit the Langmuir isotherm model, and follow the octanol–water partition law. Instead of using APRB reagent, an APRB-producing wastewater was reused to prepare the cost-effective sorbent, and the equilibrium adsorption capacities of which reached 222 and 160 mg/g for EV and BPR, respectively. The sorbents was then used to treat three wastewater samples with satisfactory results of over 97% decolonization and 88% COD-decreasing. In addition, the hybrid sorbent was regenerated from sludge over five cycles, and its adsorption capacity was not appreciably changed. This work has developed a simple and eco-friendly method for synthesizing a practical and efficient sorbent.

1. Introduction

Recently, global economic prosperity has caused rapid growth and extensive development of the textile industry. Over 100,000 dyes have been synthesized worldwide, and more than 700,000 tonnes are produced annually. More than 10,000 dyes are commercially available, but over 5% is discharged into aquatic environments by plants and users [1]. During the dye production and use, highly concentrated dye wastewater is drained into environmental water without being effectively treated, especially in developing countries. For example, many dye-producing and -using plants are located throughout the Yangtze Delta Area of China, the drinking water sources of the Yangtze River and Taihu Lake. These water bodies have been greatly harmed, badly disrupting both the normal lives of people in this region and local economic development [2,3]. Dyes are classified as follows: anionic/direct, acidic and reactive; cationic/basic; and non-ionic disperse dyes, over 80% of which are of the aromatic azo type. Such dyes are frequently used for fabrics; therefore, they are expected to be adherent, long lasting and resistant to sunlight and chemical processes. Moreover, fabric dyes should not fade through oxidation during normal washing. Therefore, such dyes are usually stable in acidic and alkaline media and resistant to temperature, heat, light and microbes [4], and that gives them the potential for persistence and long-term accumulation in the environment. Most azo dyes are toxic, carcinogenic and mutagenic, causing allergies, dermatitis, skin irritation, cancer and mutations in humans [5]. Therefore, regulation of dye discharge and dye-polluted or -colored wastewater has become increasingly stringent in many countries.

The removal, decolorization, mineralization and decomposition of azo compounds in dye wastewater are very important. In recent years, conventional abiotic techniques have been widely developed and applied in the treatment of azo dye wastewater. These techniques can be divided into separative treatments, including adsorption, flocculation, ion exchange and membrane filtration; and destructive treatments, including electrolysis, oxidation and reduction. Some of them have proved effective, but they often have serious limitations. For instance, activated carbon is the most efficient and popular adsorbent, so it is often used to treat variable wastewater [6]. However, chemical and thermal regeneration of spent carbon are both expensive and impractical on a large scale; also, they produce additional effluent and result in considerable adsorbent loss. Natural substances have also been used as sorbents, *e.g.* wood dust, bentonite and waste solids [7–10]. Adsorption by conventional sorbents generally depends on the specific surface area, so low adsorption capacity, poor selectivity, slow

Abbreviations: APRB, weak acidic pink red B; EV, ethyl violet; MB, methylene blue; WAG, weak acidic green GS; BPR, basic pink red B; ABB, acidic brilliant blue 6B; CBR, cationic brilliant red 5GN; POPs, persistent organic pollutants; Phe, phenanthrene; Flu, fluorene; Bip, biphenyl; BPA, biphenol A.

* Corresponding author. Tel.: +86 21 65988598; fax: +86 21 65988598.
E-mail address: hwgao@tongji.edu.cn (H.-W. Gao).

0304-3894/$ – see front matter © 2009 Elsevier B.V. All rights reserved.
doi:10.1016/j.jhazmat.2009.09.146

adsorption rate and difficult reproduction [11] restrict the extensive use of most sorbents. Furthermore, membrane filtration is slow and entails a high cost of use, while flocculation entails several problems, including color reversion of treated water and disposal of sludge with high water content; and destructive treatments with high cost often cause secondary pollution. Thoughtfully, the "using waste to treat waste" paradigm in the treatment of wastewater is often adopted because waste reuse is an optimal solution [12]. Recently, some wastes have been reused and applied in the treatment of dyes wastewater, such as fly ash [10,13], de-oiled soya [14], wheat husk [15] and so on [8,16], which do significant contributions to the pollution control and resource reuse partly.

There has been a great deal of interest in the design and synthesis of inorganic/organic complex materials to achieve specific properties. Various synthesis techniques developed during the last few years have given us access to functional materials with characteristics such as surface modification, inorganic/organic hybridization and functional ligand-loading [17,18]. These materials have been widely applied in various fields such as films, catalysts and pharmaceutical products [19–21]. A dye with a functional group that absorbs visible light is often used to prepare hybrid materials for application to solar cells and sensors [22,23]. However, these synthesis methods often require complicated procedures, strict conditions and high purity reagents [24].

Adsorptive precipitation was discovered during the mid 20th century and applied mostly in analytical chemistry [25]. The classical co-precipitation method has been extensively applied to the enrichment of metal ions [26] and the synthesis of functionalized materials [24]. As a conventional dyes, weak acidic pink red B (APRB) shows good electrophilicity and hydrophobicity, due to containing two negative sulfonic acid groups and a long hydrophobic alkyl chain. It attracted us whether a novel absorbent can be synthesized through co-precipitation hybrid of APRB with some appropriate inorganic skeleton. If feasible, a new idea is inspired: based on the selective of co-precipitation to some extent, concentrated APRB-producing wastewater should also be reused as a reactant to prepare a more cost-effective sorbent applicable to the treatment of organic wastewater. In this work, both of clean and waste APRB were applied as the active species and $BaSO_4$ as the skeleton to construct novel adsorbents successfully. The removal of cationic dyes and POPs indicated that it has a high adsorption capacity caused by charge attraction and hydrophobic stack. Moreover, recurrent regeneration of the sorbent by acidifying sludge was tested for reuse.

2. Experimental

2.1. Materials

The APRB reagent (content > 98%) and an APRB-producing wastewater were provided by the Zhejiang Shuanghong Chemical Plant. The dyes: ethyl violet (EV, C.I. 42600), methylene blue (MB, C.I. 52015), weak acidic green GS (WAG, C.I. 61580), basic pink red B (BPR, C.I. 50240) and acidic brilliant blue 6B (ABB, C.I. 42660) (purity > 95%) and the POPs: phenanthrene (Phe), fluorene (Flu), biphenyl (Bip) and biphenol A (BPA) (purity > 99.9%) were purchased from Sigma. The MB and cationic brilliant red 5GN (CBR, C.I. 48016) wastewaters were sampled from two dye plants, and the POPs wastewater was taken from a chemical plant. Inorganic substances, including the skeleton reactants $BaCl_2$ and Na_2SO_4, were purchased (A.R. grade) from the Shanghai Medical Group.

2.2. Synthesis of the materials

The $BaSO_4$–APRB hybrid sorbent liquid was prepared in the addition sequence: SO_4^{2-}–APRB–Ba^{2+}, with molar ratios 1.5:0.2:1. Using the same method, the $BaSO_4$–APRB surface-modified material was prepared in the sequence ethanol–SO_4^{2-}–Ba^{2+}–APRB, and the $BaSO_4$-only liquid was prepared in the absence of APRB. The solid contents of the liquids and the concentrations of APRB, Ba^{2+} and SO_4^{2-} in the material solids were determined by spectrophotometry, Inductively coupled plasma optical emission spectrometer (ICP-OES) and ion chromatography (IC) after the solids were dissolved in ethylene diamine tetraacetic acid and ammonia (EDTA–ammonia). The thermal gravity analysis (TGA) data, X-ray diffractometer (XRD) curves and scanning electronic microscopy (SEM) images of the material powders were collected, and ζ-potentials and size distributions were determined. Transmission electronic microscopy equipped with energy dispersive X-ray spectroscopy (TEM-EDX) was used to determine the distributions of different elements in the hybrid material. BPR was used to measure the isoelectric point and K_d of the hybrid material. Instead of the commercial APRB reagent, the APRB-producing wastewater was reused to prepare a cost-effective hybrid sorbent, which was used in this work to treat the wastewaters.

2.3. Adsorption of dyes and POPs

Five dye solutions, WAG, ABB, EV, MB and BPR, were treated with the material. Their rates of removal were calculated and compared with those of the corresponding untreated dye solutions. As representative cationic dyes, EV and BPR were selected for investigating the mechanism of adsorption by the material. The molar amounts of EV and BPR bound to the material were calculated. A conventional sorbent, activated carbon powder, was compared with the hybrid sorbent. The effects of pH, ionic strength and temperature on the adsorption of EV were also determined. The POPs, Phe, Flu, Bip and BPA, were used to investigate the adsorption of hydrophobic organic substances by the sorbent. The treated supernatant was measured by spectrofluorometry and the rates of POPs removal were calculated. Furthermore, their K_{pw} values were calculated, and the relationship between the K_{ow} and K_{pw} of the POPs was established.

2.4. Treatment of wastewaters and reproduction of the sorbent

Two typical MB and CBR wastewaters were sampled from two cationic dye plants and one chemical plant. The $BaSO_4$–APRB hybrid sorbent directly prepared from the APRB-producing wastewater was used to treat them. The chromaticity and chemical oxygen demand (COD) of the dye wastewaters were determined, and their rates of removal were calculated and compared. The adsorption of POPs from the chemical wastewater was evaluated by high-performance liquid chromatography (HPLC) [27]. In addition, the sludge produced during treatment of the wastewaters was collected in a strongly acidic medium to regenerate the hybrid sorbent. Five cycles of adsorption–precipitation–recovery were performed, and the efficacy of the regenerated absorbent in treating both the dye wastewaters was examined.

The details on the experimental procedures and characterization with a more detailed description have been summarized in Supporting Information (SI) File.

3. Results and discussion

3.1. Optimization of the synthesis conditions

The reactants were added in different sequences (Fig. S1 in SI). The first addition sequence, SO_4^{2-}–Ba^{2+}–APRB, was found to result in the lowest amount of APRB captured. This is because $BaSO_4$ particles were formed before the APRB was added, so APRB could only be adsorbed on the outer surface of the $BaSO_4$ particles.

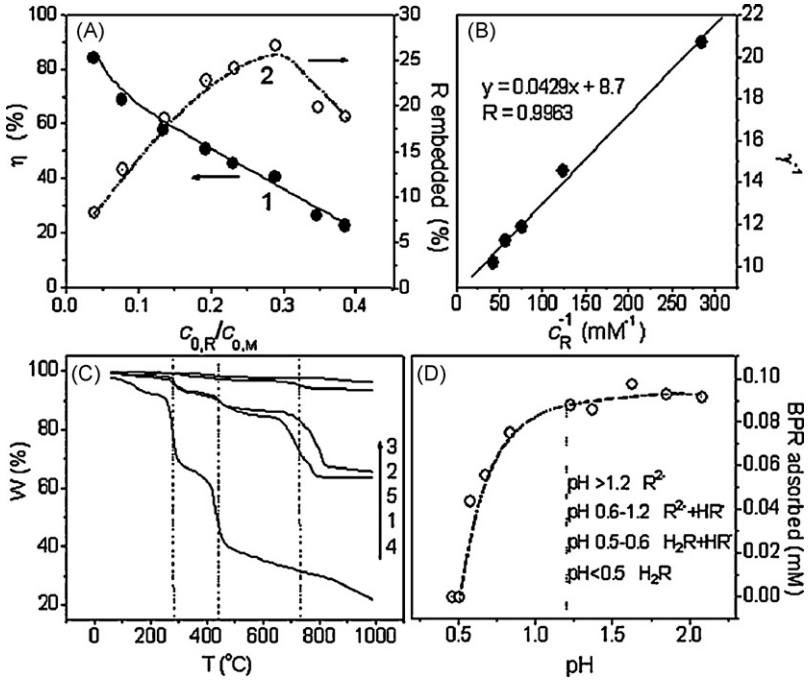

Fig. 1. (A) Variation of η (curve 1) and γ (2) of APRB embedded in $BaSO_4$ particles when 0.52 mM SO_4^{2-} ($c_{0,M}$), 0.02–0.2 mM APRB ($c_{0,R}$) and 0.73 mM Ba^{2+} was added to 30% ethanol. (B) Plots of γ vs. c_R^{-1} of the SO_4^{2-}–APRB–Ba^{2+} liquids. (C) Change in weight of the material with temperature. (1) $BaSO_4$/APRB hybrid material, (2) $BaSO_4$ (82%)–APRB (18%) mixture, (3) $BaSO_4$-only, (4) $BaSO_4$/APRB surface-modified material and (5) APRB-only. (D) Change in amount of BPR adsorbed with pH from 0.4 to 2.08 when 0.1 mM BPR was mixed with 0.025% hybrid material. The total ionic strength of each solution remained at 2 M and temperature at 20 °C.

This preparation produced an APRB surface-modified $BaSO_4$ material. The second addition sequence, Ba^{2+}–APRB–SO_4^{2-}, produced as much APRB hybrid as the first. Ba^{2+} reacted first with APRB to form a Ba–APRB complex, which has been proved no contribution to adsorbing cationic dyes. So SO_4^{2-} must competitively replace the APRB bound to the Ba^{2+}. Therefore, the sediment formed may contain a large amount of the ineffective Ba–APRB complex, weakening the adsorption capacity of hybrid material. Based on the above attempt, the third addition sequence was therefore applied, SO_4^{2-}–APRB–Ba^{2+}, which has been proved most favorable for the layer-by-layer hybridization of APRB into the growing $BaSO_4$ particles. After the APRB–SO_4^{2-}–Ba^{2+} reaction was completed, the absorption spectra of the residuary solutions (Fig. S2A) show that the amount of APRB in the hybrid particles reached a maximum in the presence of 30% ethanol. The spectra of the residuary solution (Fig. S2B) show that the gradients of the curves increased with increasing ethanol content. The increase in the slope of *log A* vs. *log λ* indicates that the number of particles decreases with increasing

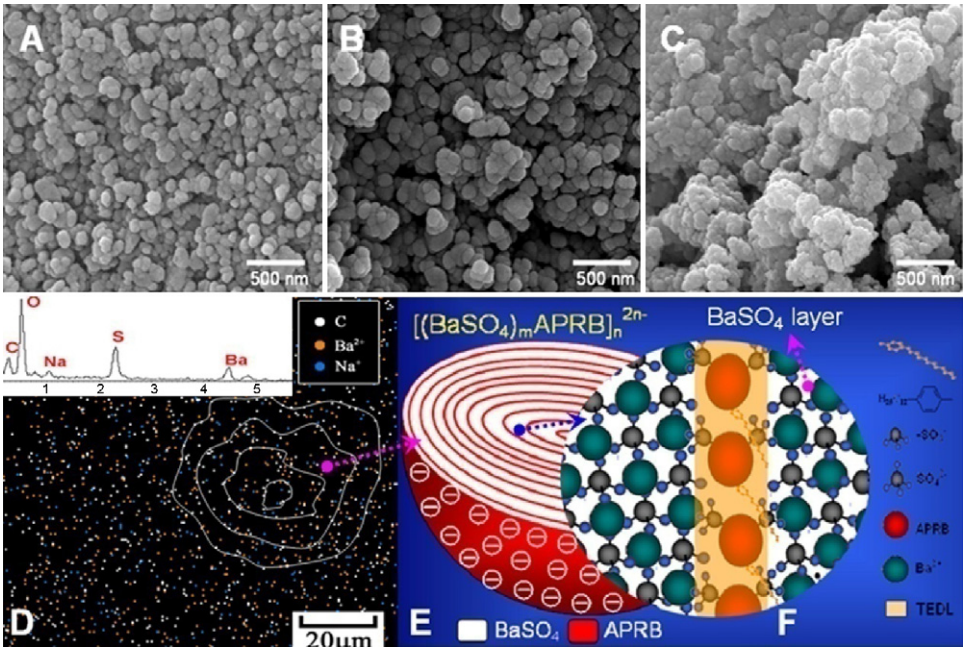

Fig. 2. SEM images of $BaSO_4$-only (A), $BaSO_4$/APRB surface-modified (B) and $BaSO_4$/APRB hybrid (C) materials. Elemental analysis and mapping of the hybrid material was conducted using TEM-EDX (D). Cartoon illustration of APRB embedded in $BaSO_4$ (E and F).

ethanol content [28]. When the ethanol concentration is over 40%, the presence of ethanol retards the growth of $BaSO_4$, and the particles become too small to settle. As a result, the amount of the settled APBR decreased at high ethanol concentrations (Fig. S2A). The number of $BaSO_4$ particles increased rapidly with increasing Ba^{2+} concentration and remained almost constant above 100 mg/L (Fig. S2C). However, the ineffective Ba–APRB complex has a solubility product (K_{sp}) of 3.1×10^{-9} (Fig. S3B); it is formed when too much Ba^{2+} is added. Thus, an initial Ba^{2+}:$SO_4{}^{2-}$ molar ratio of 1.5:1 was selected.

3.2. The formation of APRB–$BaSO_4$ hybrid particles

The precipitation of APRB (R) by Ba^{2+} and $SO_4{}^{2-}$ (M) may be expressed as the reaction:

$$N\mathrm{APRB}^{2-} + \mathrm{Ba}^{2+} + \mathrm{SO_4}^{2-} \overset{K}{\rightleftharpoons} [\mathrm{BaSO_4(APRB)}_N]^{2N-}$$

Initiation	$c_{0,R}$	$c_{0,M}$	0
Equilibrium	c_R	$c_M \to 0$	$c_{0,M}$

The symbol N is the saturating number of APRB molecules, and K is the adsorption constant. $c_{0,R}$ and $c_{0,M}$ are the initial molar concentrations of APRB and $SO_4{}^{2-}$, respectively, while c_R and c_M represent their molar concentrations at equilibrium. c_M approaches zero when the molar concentration of Ba^{2+} is higher than that of $SO_4{}^{2-}$. The molar number (γ) of APRB hybridized in the $BaSO_4$ particles is calculated by the relationship $\gamma = \eta c_{0,R}/c_{0,M}$, where the effective fraction (η) of APRB is calculated by the formula $\eta = 1 - c_R/c_{0,R}$. Both γ and η must be corrected by the Ba–APRB complex (Fig. S3A). With increasing APRB molarity, γ increases (curve 2) but η decreases (curve 1) (Fig. 1A). Regarding the effect of the initial molar ratio of APRB ($c_{0,R}$) to $SO_4{}^{2-}$ ($c_{0,M}$), the amount of hybridized APRB approached a maximum of 25% when $c_{0,R}/c_{0,M}$ was 0.25, *i.e.*, 9 $BaSO_4$ molecules can embed a maximum of 1 APRB molecule. The amount of the hybridized APRB decreases when $c_{0,R}/c_{0,M}$ is over 0.25. This is attributed to the formation of ineffective Ba–APRB particles. Therefore, the $c_{0,R}/c_{0,M}$ ratio is selected to be approximately 0.2. The Langmuir isotherm model was used to fit the experimental data, and the binding constants (N, K and the Gibbs free energy change ΔG) were calculated to be $N = 1/8.7$, $K = 2.02 \times 10^5\ \mathrm{M}^{-1}$ and $\Delta G = -30.1$ kJ/mol (Fig. 1B). Therefore, the hybridization of APRB in $BaSO_4$ particles occurred by spontaneous chemical adsorption, and the hybrid complex is very stable. APRB, containing $SO_4{}^{2-}$, may be attracted to the temporary electric double layer (TEDL) in the monolayer by its strong affinity for Ba^{2+}.

The hybridization of APRB in $BaSO_4$ particles was not influenced by pH between 2 and 9.5 (Fig. S4). This is favorable for the reuse of various APRB-producing wastewaters to obtain practical sorbents. The preparation of the hybrid material was performed in neutral media in this work.

3.3. Composition and structure of the hybrid materials

A suspension (SS) of the $BaSO_4$–APRB hybrid material was prepared under the optimal experimental conditions described above. The SS was left unstirred for 2 h, then the supernatant was removed and the solid residue of the final concentrated SS was measured as 3.5%. This was used in the succeeding experiments. The SS was dissolved in a solution of EDTA–ammonia, and the Ba^{2+} concentration was measured as 124 ± 3 μmol/mL, $SO_4{}^{2-}$ 115 ± 4 μmol/mL and APRB 10.3 ± 0.2 μmol/mL, respectively. Thus, the Ba^{2+}:$SO_4{}^{2-}$:APRB molar ratio in the hybrid material was calculated as 12:11:1. Therefore, the addition of APRB has little effect on the formation of $BaSO_4$. No covalent bonds can be formed between APRB and $BaSO_4$, so the APRB is bound by non-covalent affinity [29]. Approximately 11 $BaSO_4$ molecules occlude one APRB molecule in the working material. The excess Ba^{2+} indicates that it may be adsorbed by the solid material to maintain charge equilibrium. A cost-effective sorbent liquid prepared with an APRB-producing wastewater containing 0.074% APRB and 23,000 mg/L COD was also analyzed. The molar ratio of $BaSO_4$ to APRB was calculated as 15: 1. Slightly less APRB was hybridized than that in the hybrid material prepared with the commercial APRB reagent. The high COD value suggests that the APRB-producing wastewater may have contained unknown organic substances, *e.g.* complex byproducts and excess reactants, which may affect the hybridization of APRB in the $BaSO_4$ particles.

The TGA results from five materials, APRB-only (curve 4), $BaSO_4$-only (curve 3), $BaSO_4$–APRB mixture (curve 5), BaSO4–APRB surface-modified (curve 2) and hybrid particles (curve 1), are shown in Fig. 1C. APRB may undergo almost complete thermal decomposition below 600 °C as seen in curve 4; the weight loss was 26% around 280 °C and 27% around 430 °C (Fig. S5). The former may be caused by volatilization of the alkyl chain ($-C_{12}H_{25}$) and the latter by decomposition of the azo naphthol amide (Fig. S1). The two sulfonic groups of APRB may be transformed into sodium sulfate at 430 °C and the Na_2SO_4 into Na_2O above 650 °C. The weight loss of APRB in the $BaSO_4$ hybrid material was 10% between 200 and 450 °C according to curve 1, after correction for the $BaSO_4$-only material (curve 3). Therefore, the mass percentage of APRB was calculated as 20% in the hybrid material, *i.e.* the molar ratio of $BaSO_4$ to APRB was approximately 11. Similarly, the weight loss of APRB in the $BaSO_4$–APRB surface-modified material was only 1.2% between 200 and 450 °C, according to curve 2. Therefore, most APRB molecules were embedded in the interior of the $BaSO_4$ particles in the hybrid material. Comparing curves 3 with 5, obtained by mechanically mixing $BaSO_4$ with APRB, the weight loss tendency was quite consistent. This indicates that no covalent interaction occurred between APRB and $BaSO_4$ during preparation of the hybrid material.

Basic pink red B (BPR), a cationic dye that can exist in acidic and basic solution, was used to determine the isoelectric point of the hybrid material in order to investigate the applicability of this method. From Fig. 1D, no cationic BPR was adsorbed when the pH was less than 0.5, *i.e.*, the hybrid material carried no negative charges in a strongly acidic medium. The most likely reason is that APRB exists in the APRB-H_2 form. The dissociation constant (K_d) of APRB is $pK_d = 0.5$. The APRB forms in various pH media are shown in Fig. 1D; $APRB^{2-}$ has the highest sorption capacity for BPR. Therefore, the hybrid material is only efficient as a cationic sorbent when the pH is greater than 1.2. According to Fig. 1D, the hybrid material may be regenerated if the precipitated sludge with adsorbed cationic dye is mixed with a strongly acidic medium, *e.g.* 1 M H_2SO_4. Meanwhile, the cationic dye may be released and then concentrated highly for recovery and reuse.

The particle size analysis show that the self-aggregates of $BaSO_4$-only particles are non-uniform with sizes from 0.5 to 3 μm (Fig. S6A), and approximately 95% of the hybrid aggregates are between 0.5 and 7 μm of size (Fig. S6B). Therefore, hybridization with APRB affected the self-aggregation of $BaSO_4$ particles in size. According to the SEM images (Fig. 2A), the individual $BaSO_4$-only particles are spherical, and most are between 100 and 200 nm in diameter. The $BaSO_4$–APRB surface-modified particles are larger because of the sorption of APRB on the $BaSO_4$ particle surfaces (Fig. 2B). However, the $BaSO_4$–APRB hybrid material consists of colloid aggregates, composed of mutually bonded nanoparticles approximately 50 nm in size (Fig. 2C). The active surface of the hybrid material was not markedly exposed, and hybridization with APRB did not alter the crystallization process according to the XRD data (Fig. S7). The data show that there was no covalent interaction

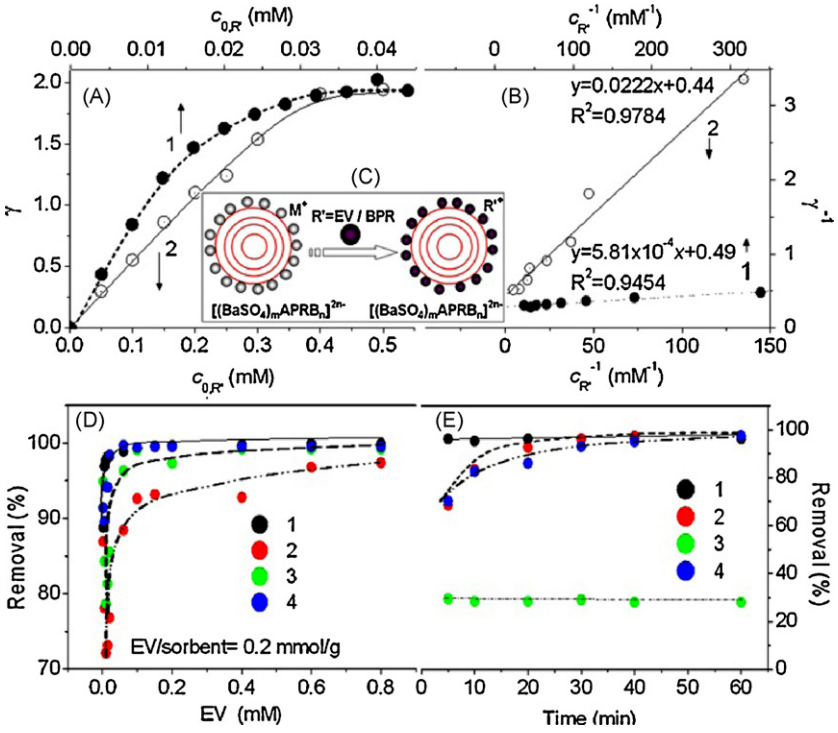

Fig. 3. (A) Plots of γ vs. c_{L0} of EV (1) and MB (2). (B) Variation in chromaticity of the EV solution after treatment with the hybrid sorbent (curve 1 at 5 min) or activated carbon powder (curve 2 at 30 min and 3 at 60 min). (C) Cartoon illustration of adsorption of cationic dye L (EV or MB) by the hybrid sorbent. (D) Variation in rate of removal of EV (initial concentration 2.0–800 μM) after treatment with the hybrid material for 2 min (curve 1) or activated carbon powder (800–1000 m^2/g SSA) for 10 min (2), 30 min (3) or 60 min (4). The ratio of EV molarity to the mass of material added was 0.2 mmol/g in each case. (E) Effect of adsorption time on the rate of removal of EV (1 and 2) (initial concentration 0.0125 mM) and BPR (3 and 4) (initial concentration 0.17 mM). Both 1 and 3 0.01% of the hybrid sorbent; 2 and 4 show the effects of treatment with 0.01% activated carbon powder.

between APRB and $BaSO_4$. Elemental analysis and element mapping of Ba, C and Na were performed by TEM-EDX (Fig. 2D). The carbon, indicating APRB (white points), is always distributed around several Ba points (yellow). This indicates that the APRB layer is sandwiched between $BaSO_4$ layers. The ratio of numbers of C to Ba atoms was calculated as 3, *i.e.* 10 $BaSO_4$ molecules interact with one APRB molecule in the working material. In addition, the Na points (blue) (Fig. 2D) indicate that Na^+ may be attracted to the hybrid particles in order to maintain the charge equilibrium with Ba^{2+}. The similar *N* values of APRB given by the various methods described above show that approximately 11 mol of $BaSO_4$ interact with only 1 mol of APRB in the working material.

In conclusion, APRB was adsorbed and then occluded in $BaSO_4$ particles, and the process of formation of a negatively charged $BaSO_4$–APRB co-precipitate is illustrated in Fig. 2E and F. In a solution containing SO_4^{2-}, APRB and Ba^{2+}, SO_4^{2-} reacts with Ba^{2+} prior to APRB because the K_{sp} (1.1×10^{-10}) of $BaSO_4$ is much less than that of the Ba–APRB complex (Fig. S3B). During the slow growth of $BaSO_4$ particles in the presence of ethanol, APRB may be adsorbed into the TEDL by the affinity between the sulfonic groups and Ba^{2+}. SO_4^{2-} immediately captures the Ba^{2+} bound to APRB and forms the outer $BaSO_4$ layer of the sphere (Fig. 2F). Thus, APRB molecules form monolayers sandwiched between $BaSO_4$ layers (Fig. 2E). In this way, many APRB layers are embedded into $BaSO_4$ particles to form a large aggregate particle with many negative charges supplied by the APRB. This is confirmed by measurement of the ζ-potential of the liquid forms of the material: -23.4 ± 0.9 mV for the hybrid material and only -7.6 ± 0.6 mV for $BaSO_4$-only. These data hint that the hybrid material can be used as an efficient sorbent to treat organic wastewater with cationic organic substances, including cationic dyes.

3.4. Adsorption of dyes and POPs

The adsorption experiments between five dyes and three kinds of materials ($BaSO_4$-only, $BaSO_4$–APRB surface-modified and $BaSO_4$–APRB hybrid materials) were carried out. As shown in Figs. S8 and S9, weak acidic green GS (WAG) was hardly adsorbed by any of the three materials due to several negative ($-SO_3^-$) groups in WAG molecule. Acidic brilliant blue 6B (ABB) was adsorbed because it carries positive ($-NR_2^+$) charges except for negative ($-SO_3^-$) group. In contrast, ethyl violet (EV), methylene blue (MB) and basic pink red B (BPR) with positive charged groups are clearly adsorbed when treated with the hybrid material. However, the $BaSO_4$–APRB surface-modified material is not very effective in adsorbing these three dyes. The $BaSO_4$-only material shows no appreciable removal of the EV, MB, BPR or WAG dyes (Fig. S9). The adsorptions of EV and MB became saturated when only 0.01% of the hybrid sorbent was added, and those of ABB and BPR increased with increasing hybrid sorbent (Fig. S9A). The selectivity of sorption showed that the interactions of cationic organic substances with the material are mainly contributed to charge attraction. Moreover, the hybrid material contains more negative charges than the surface-modified material. This again confirms that the $BaSO_4$–APRB hybrid particle will form a negative electronic aggregate in the aqueous phase.

Studies on the adsorption mechanism are a prerequisite for understanding the adsorbate–sorbent interaction so that sorbent use can be optimized. The adsorptions of EV and BPR on the $BaSO_4$–APRB hybrid material were investigated in detail. Plots of γ vs. $c_{0,R'}$, (Fig. 3A) show that the γ of EV and BPR approach a constant maximum (*N*) at 2 when their initial concentrations are greater than 0.4 mM, *i.e.* 1 mol of APRB embedded in $BaSO_4$ particles can capture only 2 mol of EV or BPR at saturation. Thus,

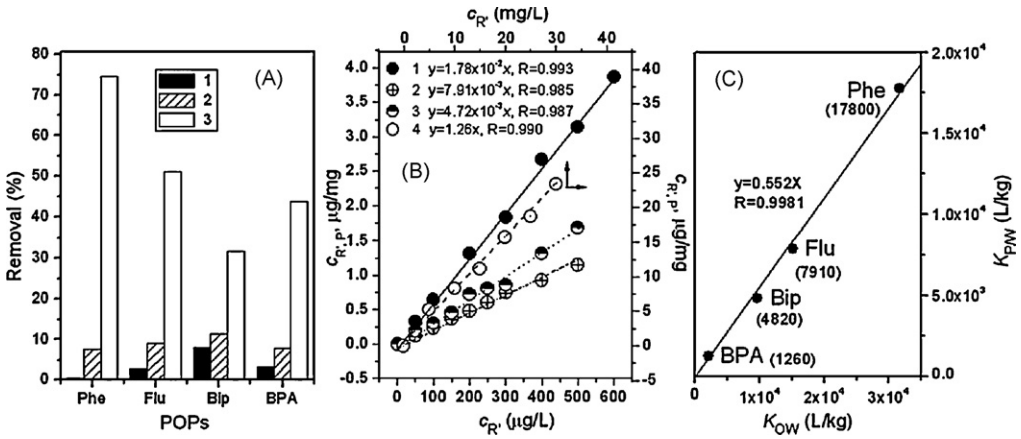

Fig. 4. (A) Rate of removal of 0.20 mg/L Phe, Flu and Bip and 10 mg/L BPA after addition of 0.01% $BaSO_4$-only (column 1), $BaSO_4$/APRB surface-modified (2) and $BaSO_4$/APRB hybrid (3) materials. (B) Plots of $c_{R',p}$ vs. $c_{R'}$ of POP solutions, initially containing 0–0.30 mg/L Phe (curve 1), 0–0.50 mg/L Flu (2), 0–0.50 mg/L Bip (3) and 0–40 mg/L BPA (4). The amounts of hybrid sorbent added were 0.01% (curves 1 and 3), 0.03% (2) or 0.05% (4). (C) The relationship between K_{pw} and K_{ow}.

the saturating mole amounts of EV or BPR neutralized all the negative charges in the hybrid particles, *i.e.* the following reaction occurred: $[(BaSO_4)_m(APRB)_n]^{2n-} + 2nR'^{+} = R'_{2n}[(BaSO_4)_m(APRB)_n]$ (R′: cationic dye *e.g.* EV or BPR, $m = 11n$) (Fig. 3C). This represents further evidence of the electronic charge pairing interaction. From the above *N* values, the adsorption capacity of the material prepared from APRB reagent was calculated to be 303 mg EV and 216 mg BPR per gram material while that of the adsorbent prepared from APRB waste to be 222 and 160 mg/g for EV and BPR, respectively. The results are obviously superior to the reported ones [30]. By deduction, APRB is the sole active agent filling the $BaSO_4$ skeleton. Furthermore, the APRB embedded in the $BaSO_4$ particle attracts oppositely charged molecules, *i.e.* the adsorption capacity of the hybrid sorbent does not correlate directly with the specific surface area (SSA) of the particles. Fitting the Langmuir isotherm model (Fig. 3B) confirmed the monolayer adsorption of EV and BPR on the hybrid material. Their *K* values were calculated as 8.43×10^5 and $2.21 \times 10^4\ M^{-1}$, respectively. EV forms a more stable complex with the hybrid material than BPR.

The effects of pH and ionic strength on the adsorption of EV were tested by treatment with the $BaSO_4$–APRB hybrid sorbent (Fig. S10). The rate of removal of EV changed little when the pH was varied between 2 and 9 and when the electrolyte was less than 1 M. The adsorption constant (*K*) of EV increased with increasing temperature, while that of BPR decreased (Fig. S11A). From the enthalpy changes (ΔH) (Fig. S11B), the adsorption of EV is endothermic while that of BPR is exothermic, which explains why increasing temperature favors the adsorption of EV but not that of BPR. The entropy changes (ΔS) indicate that the adsorption of EV on the hybrid sorbent was driven by an increase in entropy, but that of BPR was driven by enthalpy. According to the ΔG values, the adsorption of cationic dyes is generally spontaneous.

The sorption of EV and BPR on the $BaSO_4$–APRB hybrid sorbent with an SSA of only 0.89 m^2/g was compared with the classical activated carbon powder with an SSA of 800–1000 m^2/g (Fig. 3). The adsorption of EV on the $BaSO_4$–APRB hybrid material was completed in 2 min (Fig. 3D). From curves 2–4, the removal of EV treated with activated carbon becomes apparent only after vigorous mixing for 30 min. In order to overcome the capillary effect, activated carbon must be used over a long period with strong mixing [31]. Although the final rates of EV removal are similar, the hybrid material removes EV much more quickly than activated carbon. All curves in Fig. 3E point to the same conclusion. However, much less BPR is finally absorbed by the hybrid material than by activated carbon. This may be due to the saturation of the hybrid sorbent by BPR. The above observation indicates that the hybrid sorbent acts by a quite different mechanism from activated carbon. The former depends mainly on the electric charge carried, but the latter depends on the SSA.

The chemical structure of APRB is shown in Fig. S1; it has a long alkyl chain, a $-C_{12}H_{25}$ group. Thus, APRB molecules embedded on the outside surface of the material will form a hydrophobic shell that adsorbs lipophilic organic substances, *e.g.* toxic benzene derivatives and esters, and carcinogenic POPs [32]. Four polycyclic aromatic hydrocarbon (PAHs), phenanthrene (Phe), fluorene (Flu), biphenyl (Bip) and biphenol A (BPA), were used to examine the adsorption capacity of the hybrid material, and their rates of removal were calculated, as shown in Fig. 4A. POPs treated with the hybrid material were removed much more quickly than those treated with the $BaSO_4$-only and $BaSO_4$–APRB surface-modified materials. This indicates that the *in situ* chemical co-precipitation of APRB with $BaSO_4$ particles may produce a much more hydrophobic surface than surface modification with APRB. As demonstrated by the curves in Fig. 4B, the amount of POP captured does not show a constant tendency, which is very different from the case of the cationic dye (Fig. 4A). All plots of γ vs. $c_{R'}$ demonstrated good linear relationships. Therefore, the adsorption of POPs on the hybrid sorbent accorded with the octanol–water partition law; a hydrophobic interaction may occur between the long alkyl chain of APRB and the POP. The partition coefficients (K_{pw}) of the POPs in the $BaSO_4$–APRB hybrid material are given in Fig. 4C. K_{pw} is directly proportional to the corresponding K_{ow} [33] with a slope of 0.552, *i.e.* 2 g of the hybrid sorbent removes the same amount of POP as 1 g of pure octanol. The time-dependence of Phe adsorption indicates that adsorption is completed in 2 min, and temperature has no obvious effect between 10 and 40 °C.

3.5. Treatment of wastewater

Recycling and reuse of waste has long been studied in order to conserve the environment and reduce costs [12]. The $BaSO_4$–APRB hybrid sorbent was prepared directly with APRB-producing wastewater instead of commercial APRB, and it was applied to the treatment of two dye wastewaters: (1) MB wastewater with a chromaticity of 140,000 and COD = 3800 mg/L; (2) cationic brilliant red 5GN (CBR) wastewater with a chromaticity of 28,000 and COD = 1280 mg/L; and one chemical wastewater with 0.16 mg/L Phe, 0.19 mg/L Flu, 0.25 mg/L Bip and 4.0 mg/L BPA. According to Fig. 5A, the chromaticities of the two dye wastewaters clearly decreased with increasing sorbent percentage. With 1% hybrid sorbent, the decolorization was over 97% and the COD decreased by 88% (Fig. 5B). According to the changes in column

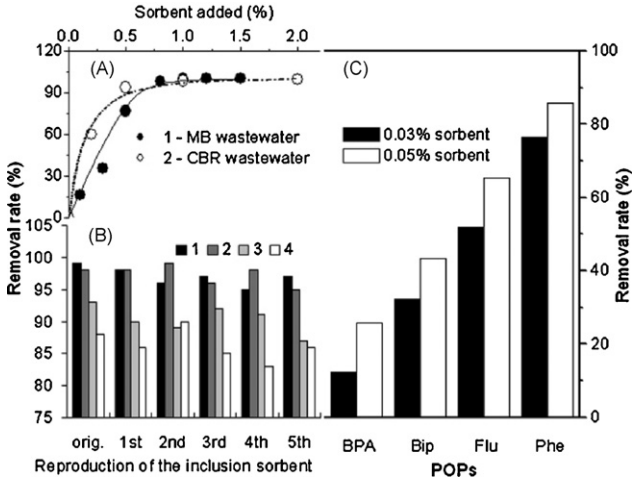

Fig. 5. (A) Changes in color of EV (1, initial chromaticity: 140,000) and CBR (2: 28,000) wastewaters with increasing amounts of $BaSO_4$/APRB hybrid sorbent directly prepared from APRB-producing wastewater. (B) Changes in chromaticity (1-EV and 2-CBR) and COD (3-EV and 4-CBR) after treatment with 1% of the original and 5-times regenerated sorbents. (C) Removal rates of POPs in chemical wastewater containing 0.16 mg/L Phe, 0.19 mg/L Flu, 0.25 mg/L Bip or 4.0 mg/L BPA, where 0.03% (black) or 0.05% (white) of the hybrid sorbent was added.

height (Fig. 5C), the rates of removal for the various POPs is correlated positively with their K_{pw} values.

The sludge that adsorbs EV and CBR dyes was collected and regenerated by the recommended procedure. The decolorization rates of both EV and CBR wastewaters were still over 95%, and the COD was decreased by more than 83% when the sorbent regenerated at each cycle was used (all 1%) (Fig. 5B). Therefore, the adsorption capacity of the recovered sorbent is not significantly different from that of the original hybrid. Moreover, only approximately 5% of the sorbent solid is lost in each recovery cycle. In contrast to conventional treatment methods, *e.g.* electrolysis and advanced oxidation, the hybrid sorbent does not destroy the structure of the cationic dye pollutant. The cationic dye adsorbed in the sludge was released and concentrated over 50-fold when the hybrid sorbent was regenerated. Thus, the cationic dye may be extracted and recovered as a useful product.

4. Conclusions

In summary, a new, highly effective sorbent was developed by the chemical co-precipitation of APRB with growing $BaSO_4$ from producing wastewater. The molar ratio of $BaSO_4$ to APRB is 11:1 in the sorbent. The nano-sized $BaSO_4$–APRB aggregate particles carry many negative charges and lipophilic groups. The efficient removal of EV, MB and BPR and of four kinds of POPs, and treatment of relevant wastewaters, indicated that the hybrid material has a very high adsorption capacity. The adsorption of cationic dyes corresponded to the Langmuir isotherm model and involved charge attraction, and that of POPs corresponded to the octanol–water partition law and involved hydrophobic stacking. The skeleton reactants are readily available and harmless to the environment. Reuse of dye wastewater and simple and easy regeneration of the hybrid sorbent from sludge saves on production and usage costs of an efficient sorbent. The sludge adsorbing various dyes may also be reused as a color paste in rubber, plastic, paint and paper-making industries. Not only has the recommended method allowed both acidic and basic dye wastewaters to be treated synchronously, but the cationic dye adsorbed was also concentrated for recovery and recycling during regeneration of the hybrid sorbent. This work has developed a simple, eco-friendly and practical method for the synthesis of an efficient and cost-effective sorbent, and it can be used to solve problems resulting from conventional flocculants such as color reversion of treated water, large volumes of sludge, and secondary pollution.

Acknowledgements

We thank the State Key Laboratory Foundation of Science and Technology Ministry of China (Grant No. PCRRY09008), the National Key Technology R&D Program of China (No. 2008BAJ08B13) and China Postdoctoral Science Foundation (No. 20080440646) for financially supporting this work.

Appendix A. Supplementary data

Supplementary data associated with this article can be found, in the online version, at doi:10.1016/j.jhazmat.2009.09.146.

References

[1] G. McMullan, C. Meehan, A. Conneely, N. Kirby, T. Robinson, P. Nigam, I.M. Banat, R. Marchant, W.F. Smyth, Microbial decolorization, degradation of textile dyes, Appl. Microbiol. Biotechnol. 56 (2001) 81–87.
[2] M. Yang, J.W. Yu, Z.L. Li, Z.H. Guo, M. Burch, T.F. Lin, Taihu lake not to blame for Wuxi's woes, Science 319 (2008) 158–1158.
[3] L. Guo, Doing battle with the green monster of Taihu lake, Science 317 (2008) 1166–11166.
[4] M.A. Talarphoshti, T. Donnelly, G.K. Anderson, Colour removal from a simulated dye wastewater using a two-phase anaerobic packed bed reactor, Water Res. 35 (2001) 425–432.
[5] A.C. Halbower, B.F. Fouty, K.A. Fagan, V. Balasubramaniam, A.W. Pike, P.V. Fennessey, M. Moss, Systemic absorption of food dye in patients with sepsis, New Engl. J. Med. 343 (2000) 1047–1053.
[6] V. Gómeza, M.S. Larrechia, M.P. Callao, Kinetic and adsorption study of acid dye removal using activated carbon, Chemosphere 69 (2007) 1151–1158.
[7] G. Crini, P.M. Badot, Application of chitosan, a natural aminopolysaccharide, for dye removal from aqueous solutions by adsorption process using batch studies: a review of recent literature, Prog. Polym. Sci. 33 (2008) 399–447.
[8] G. Crini, Non-conventional low-cost adsorbents for dye removal: a review, Bioresour. Technol. 97 (2006) 1061–1085.
[9] S. Wang, H.M. Ang, T.O. Tadé, Novel applications of red mud as coagulant, adsorbent, catalyst for environmentally benign processes, Chemosphere 72 (2008) 1621–1635.
[10] S. Wang, H. Wu, Environmental-benign utilisation of fly ash as low-cost adsorbents, J. Hazard. Mater. 136 (2006) 482–501.
[11] T. Robinson, G. McMullan, R. Marchant, P. Nigam, Remediation of dyes in textile effluent: a critical review on current treatment technologies with a proposed alterna, Bioresour. Technol. 77 (2001) 247–255.
[12] W.Z. Liu, F. Huang, Y.Q. Liao, J. Zhang, G.Q. Ren, Z.Y. Zhuang, J.S. Zhen, Z. Lin, C. Wang, Treatment of Cr^{VI}-containing $Mg(OH)_2$ nanowaste, Angew. Chem. Int. Ed. 47 (2008) 5619–5622.
[13] G.S. Gupta, G. Prasad, V.N. Singh, Removal of chrome dye from aqueous solutions by mixed adsorbents: fly ash and coal, Water Res. 24 (2009) 45–50.
[14] V.K. Guptaa, A. Mittalc, A. Malviyac, J. Mittalc, process development for removal and recovery of metanil yellow by adsorption on waste materials—bottom ash and de-oiled soya, J. Hazard. Mater. 151 (2008) 834–845.
[15] V.K. Gupta, R. Jain, S. Varshney, Removal of Reactofix golden yellow 3 RFN from aqueous solution using wheat husk—an agricultural waste, J. Hazard. Mater. 142 (2007) 443–448.
[16] V.K. Gupta, D. Mohan, S. Sharma, M. Sharma, Application of low cost adsorbents for dye removal—a review, J. Environ. Manage. 90 (2009) 2323–2342.
[17] S. Mintova, V.D. Waele, U. Schmidhammer, E. Riedle, T. Bein, In situ incorporation of 2-(2-hydroxyphenyl)benzothiazole within FAU colloidal crystals, Angew. Chem. Int. Ed. 42 (2003) 1611–1614.
[18] J. Genzer, K. Efimenko, Creating long-lived superhydrophobic polymer surfaces through mechanically assembled monolayers, Science 290 (2000) 2130–2133.
[19] C. Sourisseau, Polarization measurements in macro- and micro-Raman spectroscopies: molecular orientations in thin films, azo-dye containing polymer systems, Chem. Rev. 104 (2004) 3851–3892.
[20] C.J. Zhong, M.M. Maye, Core–shell assembled nanoparticles as catalysts, Adv. Mater. 13 (2001) 1507–1511.
[21] R. Karinaga, Y. Jeong, S. Shinkai, K. Kaneko, K. Sakurai, Embedment of DNA into organic gelator fibers made of amphipathic molecules, its controlled release, Langmuir 21 (2004) 9398–9401.
[22] Q.F. Zhang, T.P. Chou, B. Russo, S.A. Jenekhe, G.Z. Cao, Aggregation of ZnO nanocrystallites for high conversion efficiency in dye-sensitized solar cells, Angew. Chem. Int. Ed. 47 (2008) 2402–2406.
[23] M. Bruchez, M. Moronne, P. Gin, S. Weiss, A.P. Alivisatos, Semiconductor nanocrystals as fluorescent biological labels, Science 281 (1998) 2013–2015.
[24] I. Potapova, R. Mruk, C. Hübner, R. Zentel, T. Basché, A. Mews, CdSe/ZnS nanocrystals with dye-functionalized polymer ligands containing many anchor groups, Angew. Chem. Int. Ed. 44 (2005) 2437–2440.

[25] M.L. Baumann, A.L. Hatmaker, Ultramicro-, micro-determination of chloride by argentimetric titration with the indicator dichiorofluorescein, Clin. Chem. 7 (1961) 256–263.
[26] M. Tuzena, D. Citaka, M. Soylak, 5-Chloro-2-hydroxyaniline-copper(II) coprecipitation system for preconcentration, separation of lead(II), chromium(III) at trace levels, J. Hazard. Mater. 158 (2008) 137–141.
[27] Y. Liu, L. Chen, J.F. Zhao, Q.H. Huang, Z.L. Zhu, H.W. Gao, Distribution, sources of polycyclic aromatic hydrocarbons in surface sediments of rivers, an estuary in Shanghai, Environ. Pollut. 154 (2008) 298–305.
[28] H.W. Gao, M.H. Mou, J.F. Zhao, Spectrophotometric determination of suspending solid in natural water, Asian J. Chem. 11 (1999) 1556–1558.
[29] H.W. Gao, J.F. Zhao, Q.Z. Yang, X.H. Liu, L. Chen, L.T. Pan, Non-covalent interaction of 2′, 4′, 5′, 7′-tetrabromo-4,5,6,7-tetrachloro-fluorescein with proteins, its application, Proteomics 6 (2006) 5140–5151.
[30] W.T. Tsai, Y.M. Chang, C.W. Lai, C.C. Lo, Adsorption of ethyl violet dye in aqueous solution by regenerated spent bleaching earth, J. Colloid Interface Sci. 289 (2005) 333–338.
[31] A. Baçaoui, A. Dahbi, A. Yaacoubi, C. Bennouna, F.J. Maldonado-Hódar, J. Rivera-Utrilla, F. Carrasco-Marín, C. Moreno-Castilla, Experimental design to optimize preparation of activated carbons for use in water treatment, Environ. Sci. Technol. 36 (2002) 3844–3849.
[32] J.A. Arnot, D. Mackay, Policies for chemical hazard, risk priority setting: can persistence, bioaccumulation, toxicity, quantity information be combined, Environ. Sci. Technol. 42 (2008) 4648–4654.
[33] X.L. Qu, X.R. Wang, D.Q. Zhu, The partitioning of PAHs to egg phospholipids facilitated by copper, proton binding via cation–π interactions, Environ. Sci. Technol. 41 (2007) 8321–8327.